Graphene Nanofiber-Based Composites for Fuel Cell Application

Benalia Kouini and Hossem Belhamdi

Abstract Graphene is becoming very important in recent years, due to its interesting electrical, thermal, mechanical, and electrochemical properties. With these advantages, graphene has been used as a substance to incorporate various kinds of functional materials. Among them, graphene-based polymer nanocomposites have attracted a great deal of interest due to their new properties or enhanced performance during the last few years. This is because graphene-based polymer nanocomposites are used for electronic, optical, and electrochemical applications owing to their advantages. This chapter review discusses the preparation methods of graphene-polymer nanocomposites, some examples of graphene/polymer composites, the electrochemical behavior of graphene, and summarizes the recent research and development on Graphene nanofiber-based composites fuel cells.

1 Introduction

Graphene, a form of carbon experimentally demonstrated in 2004, [1] consists of a monolayer of carbon atoms sp^2 bonded into a two-dimensional sheet. Graphene is a basic building block for graphitic materials of all other dimensionalities as illustrated in Fig. 1 Graphene possesses unique electronic properties, including ambipolar electric field effect, extremely high mobility of charge carriers (up to 105 $cm^2\ V^{-1}\ s^{-1}$), mass-less electron, quantum Hall effects (QHE) even at room temperature, and electron wave propagation within a one atom thick layer [2, 3]. The unique properties of graphene have sparked widespread interest and investigations

B. Kouini (✉)
Laboratory of Coatings, Materials and Environment, M'Hamed Bougara University, 35000 Boumerdes, Algeria
e-mail: kouinib@univ-boumerdes.dz

H. Belhamdi
Research Unit: Materials, Processes and Environment (RU/MPE), M'Hamed Bougara University, 35000 Boumerdes, Algeria
e-mail: h.belhamdi@univ-boumerdes.dz

S. K. Tiwari et al. (eds.), *Electrospinning of Graphene*, Carbon Nanostructures,
https://doi.org/10.1007/978-3-030-75456-3_6

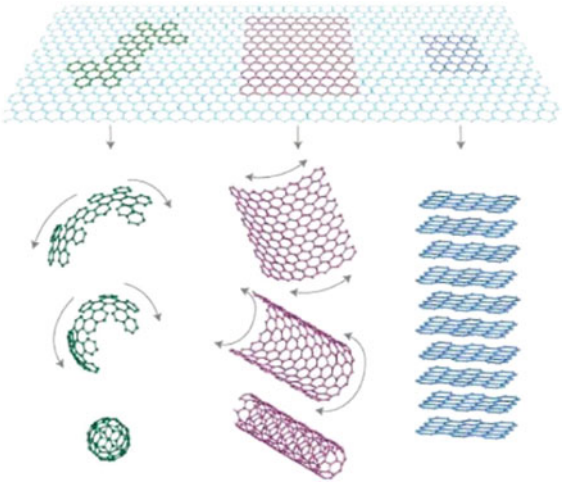

Fig. 1 Graphene is the building block of all graphitic forms: 0-dimensional buckyballs, 1-dimensional carbon nanotube, or 3-dimensional graphite (Reproduced with permission from ref [2]. Copyright 2007, Springer Nature)

in laboratories around the world. But despite the surge in interest, the chemical and physical understanding of graphene is still evolving as are the potential applications.

Graphene shows a very high surface area (B2600 m^2 g^{-1}), much larger than the surface areas of graphite (B10 m^2 g^{-1}) and carbon nanotubes (1300 m^2 g^{-1}) [4]. These remarkable properties make graphene promising in applications such as polymer-composite materials, [4, 5] paper-like materials, [6] photo-electronics, [7–9] field-effect transistors, [10] electromechanical systems, [11, 12] sensors and probes, [13–15] hydrogen storage, [16] and of course electrochemical energy systems [17].

Also, the discovery of graphene with its combination of extraordinary physical properties and the ability to be dispersed in various polymer matrices has created a new class of polymer nanocomposites [18].

One of the most common graphene-based nanocomposites is graphene-based polymer nanocomposites, which show superior thermal, electrical, mechanical, optical, and electrochemical properties compared with the neat polymer or graphene. Therefore, graphene-based polymer nanocomposites are intensively explored in applications such as supercapacitors, sensing platforms, fuel cells, solar cells, and so on [19].

2 Preparation Methods of the Graphene-Polymer Nanocomposites

The properties of graphene-based polymer nanocomposites are dependent upon the processing conditions in the fabrication of graphene/polymer nanocomposites. The functionality of graphene components is critical to lower filler loading rate, make them highly dispersed and organized sheets within a polymer matrix to enhance the

properties of nanocomposites. In particular, the mechanical properties depend on the specific surface area, aspect ratio, organization, and loading content of graphene materials. The dispersion, interfacial strength, affinity of components, and spatial organization are all of great importance in determining the final stiffness, strength, toughness, and elongation of polymer nanocomposites under various loading conditions [20–24]. The pretreatment procedures and the fabrication methods control the fine morphology and physical/chemical properties of graphene-based polymer nanocomposites. For various graphene-polymer nanocomposites known to date, the extent of dispersion and exfoliation of graphitic layers is controlled by the applied shear force, temperature, and solvent polarity. Effective control of restacking, wrinkling, and aggregation of graphene sheets is required for the development of functional nanocomposites with high performance. Extremely flexible and high-aspect-ratio graphene components are prone to random wrinkling, buckling, or folding during processing, which dramatically affects the ultimate performance. In the case of the post-treatment, the degree of dispersion can be further influenced by the hydrophobic nature of reduced graphene oxide sheets and dewetting processes at the interfaces.

The choice of fabrication methods is determined by the surface functionalization of integrated graphitic sheets. Generally, traditional fabrication routines include solution-based processing [25–28] and melt-based processing [29–31]. Among the most popular approaches for chemical modification and assembly are in-situ polymerization, chemical grafting, latex emulsion blending, layer-by-layer (LbL) assembly, and directed assembly [25, 26, 32–34]. For the in-situ polymerization method, intercalated monomers within expanded graphite clusters can promote their efficient exfoliation into single sheets throughout the polymer matrix caused by catalysis reactions [27].

Solution processing maximizes filler dispersion in a polymer matrix by using pre-suspended single-layered graphene sheets. Different solvents (aqueous to organic) can be used to dissolve graphene materials, including graphene oxide and reduced graphene oxide materials. This approach has been widely exploited due to its high dispersion efficiency, facile and fast fabrication step, and a high level of control on component behavior. By the way, melt-based mixing is a solvent-free process in which applied mechanical shear force distributes the fillers in the polymer matrix using a screw extruder or a blending mixer [28, 35]. This method allows stacked graphite or reduced graphene oxide sheets to be exfoliated into a viscous polymer melt by suppressing unfavorable interactions and inducing component dispersion. Melt mixing is recognized as a practical approach that can be adapted to graphene-based polymer nanocomposites.

3 Examples of Graphene/Polymer Composites

3.1 Graphene/Epoxy Composites

Graphene has been incorporated into epoxy-based materials to enhance various functional properties. Graphene's excellent mechanical properties make it is a good candidate for reinforcement in nanocomposites. Bortz et al. [36] investigated the effect of graphene concentration on the mechanical properties of graphene/epoxy nanocomposites. The tensile modulus of unmodified epoxy increased by ≈12% at only 0.1 wt.% loading of graphene oxide. Wajid et al. [37] used solution mixing to fabricate graphene/epoxy composites. The strength and modulus increased by 38 and 37% respectively at only 0.46 vol% graphene loading. By using a simple solution mixing technique, Galpaya et al. [38] fabricated a graphene oxide/epoxy nanocomposite with enhanced mechanical properties. At only 0.1 wt.% additionof graphene oxide, fracture toughness increased by ≈50%. The graphene oxide sheets in the composite disturbed and deflected the crack propagation. The elastic modulus increased by ≈35% from the neat epoxy with only 0.5 wt.% loading of graphene oxide. Shen et al. [39] investigated the tribological properties of epoxy nanocomposites reinforced with graphene oxide at low loading (0.05–0.5 wt.%). The wear resistance significantly increased with the addition of graphene oxide, such that, at 0.5 wt.% loading, the specific wear rate was reduced by 90.0–94.1% compared to the neat polymer.

Electrical conductivity in nanocomposites is achieved by the formation of a continuous network of the conductive fillers [40, 41]. Therefore, because graphene has a very high-aspect-ratio, the percolation threshold is achieved at very low graphene loading [42]. Wajid et al. [37] used sonication and shear mixing methods to disperse graphene into the epoxy matrix and achieved the percolation threshold at 0.088 vol%. In another study, the composites were fabricated by the incorporation of functionalized graphene into the epoxy matrix by an in-situ process. The percolation threshold was reached only after 0.52 wt.% loading of graphene, and electrical conductivity increased from 1^{-10} to 1^{-2} S cm^{-1} by ≈9 vol% loading of reduced graphene oxide. Zhao et al. [43] conducted a thorough investigation into the properties of epoxy composite filled with epoxide-functionalized graphene (G-EP). The tensile strength and Young's modulus increased by 116% and 96%, respectively, compared to the polymer at only 1 wt.% loading of G-EP. The percolation threshold was reached at only 0.33 wt.% loading, and electrical conductivity increased from about 1^{-17} to 1^{-2} S $^{cm-1}$ at ≈2 vol% loading. Thermal conductivity also improved by 189% at 10 wt.% G-EP loading. For a more comprehensive review of graphene/epoxy nanocomposites, the reader is referred to a review by Rasheed et al. [44].

3.2 Graphene/Cellulose Composites

Graphene has been incorporated in cellulose composites to enhance mechanical and electrical properties. GO and cellulose was dissolved in N-methyl morpholine-N-oxide (NMMO) monohydrate to prepare the composite films [45]. Despite being brittle, the produced graphene/cellulose composites showed improved thermal and electrical properties. Nguyen et al. [46] used reduced graphene oxide sheets (RGO) and amine-modified nano fibrillated cellulose (A-NFC) to produce composites with enhanced properties. These composites showed good electrical conductivity of up to 71.8 Sm^{-1} and tensile strength of up to 273 MPa. Graphenecellulose paper (GCP) membranes are used to fabricate flexible supercapacitors [47]. These composites displayed high electrical conductivity stability with a decrease of only 6% after being bent 1000 times. The capacitance of these supercapacitors per geometric area is 81 mF cm^{-2}, which is equivalent to a gravimetric capacitance of 120 F g^{-1} of graphene, and these supercapacitors did not lose any capacitance after 5000 cycles. Manman et al. [48] reported cellulose/graphene composite hydrogels prepared from ionic liquids (IL). They used Vitamin C to prepare RGO directly in IL. These hydrogels showed enhanced mechanical and thermal properties. At only 0.5 wt.% doping of RGO in cellulose composite, Young's modulus was improved more than four times.

3.3 PVA/Graphene Nanocomposites

Zhao et al. [49] reported the preparation of graphene nanosheets and poly (vinyl alcohol) (PVOH) via a facial aqueous solution. In their study, they showed that Graphene, flat carbon nanosheets, has generated huge activity in many areas of science and engineering due to its unprecedented physical and chemical properties. With the development of wide-scale applicability including facile synthesis and high yield, this exciting material is ready for its practical application in the preparation of polymer nanocomposites. Here they have reported that nanocomposites based on fully exfoliated graphene nanosheets and poly (vinyl alcohol) (PVA) are prepared via a facial aqueous solution. Significant enhancement of mechanical properties of the graphene/PVA composites is obtained at low graphene loading; that is, a 150% improvement of tensile strength and a nearly 10 times increase of Young's modulus are achieved at a graphene loading of 1.8 vol %. The comparison between the experimental results and theoretical simulation for Young's modulus indicates that the graphene nanosheets in the polymer matrix are mostly dispersed randomly in the nanocomposite films. Liang et al. [50] also studied poly (vinyl alcohol) (PVOH)/-graphene nanocomposites. In this study, they used water as a solvent to fuse GO into the PVOH matrix. At only 0.7 wt.% GO loading, tensile strength increased by 76%, and Young's modulus by 62%.

3.4 Polyurethane (PU)/Graphene Composites

Lee et al. [51] reported the study of waterborne polyurethane (WPU)/graphene sheets (FGS) nanocomposites prepared using an in-situ method. The electrical conductivity of the nanocomposites was increased 10^5-fold compared with that of pure WPU. This was attributed to the high dispersity and homogeneity of graphene sheets in the WPU matrix. They obtained a percolation threshold of graphene sheets at only 2 wt.%. Liang et al. [52] used thermoplastic polyurethane (TPU) to fabricate nanocomposites with three differently processed graphene samples. They were able to show that the rate of thermal degradation for thermoplastic polyurethane/isocyanate modified graphene composites are much higher than that of the sulfonated graphene and reduced graphene-based TPU nanocomposites. The TPU/-graphene nanocomposites doped with only 1 wt.% sulfonated graphene showed enhanced infrared-triggered actuation performance. The tests showed that the composite could contract and lift a 21.6 g weight up to 3.1 cm with 0.21 N of force when exposed to IR. The mechanical properties of this composite were also increased. The tensile strength of TPU/sulfonated graphene nanocomposites with 1 wt.% graphene was increased by 75% at a strain of 100%, and Young's modulus was enhanced by 120% [52]. However, IR-triggered actuation performance of isocyanate modified graphene/TPU nanocomposites showed inferior results.

3.5 Graphene/Polyethylene Terephthalate (PET) Nanocomposites

The melt intercalation technique was used to prepare PET/-graphene composites by Zhang et al. [53] Transmission electron microscopy analysis showed that graphene nanosheets were evenly distributed in the PET matrix. This criterion was confirmed by the high electrical conductivity values they got from the PET/-graphene composites. The threshold percolation was only 0.47 vol% loading and with graphite 2.4 vol%. The high electrical conductivity of 2.11 Sm^{-1} was achieved with the addition of only 3.0 vol% graphene.

3.6 Polycarbonate (PC)/Graphene Nanocomposites

Kim et al. [54] studied PC composites doped with graphite and functionalized graphene sheets (FGS) by the melt intercalation technique. In this study, they used melt rheology to study the viscoelastic properties of the composites. They annealed the composites for 10,000 s and observed that the composites manifest a solid-like state above the percolation threshold, which was around 1 wt.% for the FGS, while around 3 wt.% for graphite loading. In terms of electrical properties, FGS/PC showed

a lower percolation threshold as compared to graphite/PC composites. Both graphite and FGS fillers lead to improved PC composites stiffness and dimensional stability. The composites also exhibited good barrier properties. The permeability of nitrogen and helium of the PC composites is significantly reduced by the incorporation of both FGS and graphite. Moreover, FGS showed potential for application in gas separation processes as it was more effective against molecules with large kinetic diameters.

3.7 Polystyrene (PS)/Graphene Nanocomposites

Polystyrene/graphene composites have been extensively studied for various applications. Stankovich et al. [55] reported PS/isocyanate modified graphene composites prepared using a solution blending method in DMF. They obtained a percolation threshold for the electrical conductivity at 0.1 vol% GO in PS. The low percolation value is due to the homogeneous dispersion and an extremely large aspect ratio of graphene sheets. The PS/graphene composite showed an electrical conductivity of $\approx$0.1 to $\approx$1 Sm^{-1} at 2.5 vol% loading. Liu et al. [56] prepared a PS/GNP composite in ionic liquids. The electrical conductivity increased from 10^{-14} Sm^{-1} for pure PU to 5.77 Sm^{-1} with the addition of 0.38 vol% GNP, which is 3–15 times higher than that of polystyrene composites filled with single-walled carbon nanotubes. They also studied the thermal stability of PS/GNP composite and pure polystyrene. The degradation temperature of the PS/GNP composite was about 50 °C higher than that of pure PS. This enhancement is due to the strong interaction of GNP and the polymer matrix at the interface, which leads to a decrease of polymer chain mobility near the interface and, hence, the increase in thermal stability.

3.8 Other Graphene-Based Polymer Nanocomposites

Poly (ε-caprolactone) (PCL)/graphene oxide composite was prepared using in-situ polymerization [57]. The resulting nanocomposite shows excellent mechanical properties and robustness under bending. Poly (lactic acid) (PLA)/graphene nanocomposites were prepared using the response surface method [58], which showed that graphene loading had a significant effect on tensile strength. Liu et al. [59] fabricated graphene oxide (GO) reinforced epoxy resin nanocomposite by transferring GO from water to acetone. Incorporation of _1 wt.% of graphene oxide showed a significant improvement in flexural strength, flexural modulus, impact strength, and storage modulus. Mohamadi et al. prepared polymethyl methacrylate (PMMA)/graphene nanocomposite by sing in-situ polymerization [60]. Liang et al. fabricated polydiacetylene (PDA)/graphene nanocomposite by solution processing method [61]. The resulting nanocomposite showed excellent actuation character with controllable motion, fast response rate, and high-frequency resonance. Polyphenylene sulfide

(PPS)/graphene composite was prepared by the spraying method [62]. The resulting nanocomposite had seven times higher wear life than that of neat PPS.

Pang and his co-workers reported a novel conductive ultrahigh-molecular-weight polyethylene (UHMWPE) composite with a segregated and double percolated structure containing high-density polyethylene (HDPE) as carrier polymer for graphene nanosheets (GNS) [63].

4 Graphene-Based Electrochemical Energy Devices

Junbo Hou et al has well developed Graphene-based electrochemical energy devices [64]. The electrochemistry of graphene has been systematically investigated concerning surface chemistry and structure, heterogeneous charge transfer rate constants on redox species, electrochemical operating window, and electrocatalysis of molecules [65, 66]. The most notable feature of graphene is the very large electrochemically active surface area. Cyclic voltammetry shows 13 times higher capacitance on the graphene electrode than that on the bare glassy carbon (GC) [65]. Calculated from chronocoulometric curves at different electrodes for the reduction of 1 mM $K_3Fe(CN)_6$ with 2 M KCl, the area for different electrodes is graphene/GC ($0.092\ cm^2$) > GC electrodes ($0.0706\ cm^2$) > graphite/GC ($0.0560\ cm^2$) [66]. Besides the very large physical surface area, the sp2-hybridized structure may contribute to the high capacitance value particularly for graphene. Finally, as with other carbon allotropes, [67], significant edge-plane-like defective sites are existing on the surface of graphene.

Several systems including $Ru(NH_3)_6^{3+/2+}$, $Fe(CN)_6^{3-/4-}$ $Fe^{3+/2+}$, and dopamine (DA) have been used for testing the electrochemistry of graphene because of their well-known sensitivity and selectivity to the electronic properties, surface microstructure, and surface chemistry of carbon electrodes [65, 67]. Voltammograms of these redox systems demonstrate fast charge transfer kinetics on a graphene electrode. Electrochemical impedance spectroscopy (EIS) shows that the graphene electrode possesses smaller charge transfer resistance compared with the graphite/GC and GC electrodes. In addition to its favorable surface characteristics, the electrochemical operating window for a graphene electrode in 0.1 M pH 7.0 PBS is 2.5 V, which is comparable to that for graphite and GC electrodes [66]. Finally, graphene prepared from graphite generally does not contain any heterogeneous impurities which are a significant advantage over CNTs [68]. The following sections discuss the implications of these and other graphene characteristics for electrochemical device applications including fuel cells, supercapacitors, and batteries.

4.1 Fuel Cells

Polymer electrolyte membrane (PEM) fuel cells are electrochemical energy conversion devices, which have attracted considerable interest as power sources for mobile and stationary applications, with active research and development programs all over the world focused on this field in recent decades [69, 70]. However, despite this effort, the cost and durability issues related to the materials and components still hinder the commercialization of PEM fuel cells. Graphene sheets, with their unique nanostructure and properties, are promising alternatives for several of the critical PEM fuel cell materials. As a carbon allotrope, the most obvious use for graphene is as catalyst support. Generally, the catalyst support materials should have particular properties such as (i) high specific surface area, improving the dispersion of catalytic metals, (ii) chemical stability under oxidative and reductive conditions at relevant temperatures (150 °C or less for PEM fuel cells), (iii) high electrochemical stability under fuel cell operating conditions, (iv) high conductivity, and (v) easy recovery of Pt in the used catalyst [71].

For porous electrodes, such as those employed in PEM fuel cells, the specific surface area of the catalyst support is a critical factor. For graphene, the theoretical specific surface area of graphene is about 2600 $m^2\ g^{-1}$, but the specific area of multilayer graphene decreases. The limiting case is graphite, having a specific surface area of only 10 $m^2\ g^{-1}$. If the graphene-supported catalysts are prepared in one step, the chemical reductions of graphene oxide and the metal salts occur simultaneously. With this process, there are most likely single-, double-, and few-layer graphene sheets as well as thin graphite films co-existing in the resulting supported catalyst. Thus, the actual specific surface area of the supported catalysts will be far below the theoretical value. Even so, the produced catalysts exhibit high electrocatalytic activity [72–74].

In addition to the active surface area, the durability of the catalyst and the support is an important issue in fuel cell applications. There are two ways by which the catalyst surface area is lost. One is coalescence sintering in which two catalyst clusters touch, and then fuse into one larger cluster.

The other is Ostwald ripening in which atoms evaporated from one cluster transfer to another, creating one larger cluster [71]. Coalescence sintering is enhanced by carbon corrosion which occurs under a high potential and acid environment (i.e., the PEM fuel cell condition). In this process, the carbon support is oxidized into CO_2 or CO causing the catalyst support to collapse and thus causing coalescence sintering. Also, when the carbon support is oxidized into surface oxygen-containing species, the catalyst–carbon interactions will be weakened also facilitating coalescence sintering. Graphene may improve catalyst durability by providing a more stable support material and by strengthening the interaction of the catalyst with the support.

Finally, a high-performance PEM fuel cell electrode requires the formation of numerous triple-phase boundaries (TPBs) to create efficient reaction sites at nanoscale or microscale. The TPB is accessible for mass transfer (reactants and

products), protons, and electrons, and provides a site where electrochemical reactions can occur. The microstructure of the typical catalyst layer in the PEM fuel cells can be depicted as catalyzed carbon particles flooded with the electrolyte to form agglomerates covered with a thin film of electrolyte. The reactant gas first passes through the channels between the agglomerates, diffuses through the ionomer thin film and thereafter in the agglomerates, and then reaches the TPBs [75].

There are two main pore structures: the primary pores in the agglomerates with characteristic lengths on the order of nanometers or tens of nanometers; and the secondary pores between agglomerates with characteristic lengths from nanometer to a micrometer. These pore structures are essential for gas and water transport. The unique planar geometry of graphene coupled with its high electrical conductivity provides an opportunity to create particularly promising TPB architectures.

Research efforts to take advantage of the unique features of graphene to produce supported catalysts with enhanced activity, increased durability, and high-performance electrode architectures are discussed in the following sections.

4.1.1 Enhanced Electrocatalytic Activity

The prospect for enhanced fuel cell catalysts using a high specific surface area graphene support was explored by preparing graphene–metal particle nanocomposites [72]. This work demonstrated that graphene oxide can be reduced by ethylene glycol (EG), and thus, graphene–metal particle nanocomposites can be prepared in one step in the water-EG system using graphene oxide as a precursor with metal nanoparticles (Au, Pt, and Pd). This approach has the additional advantage that the metal nanoparticles can be adsorbed on graphene oxide sheets and thus facilitates the catalytic reduction of graphene oxide with EG. The cyclic voltammogram of methanol oxidation on the prepared graphene–Pt nanocomposites demonstrate the potential application in direct methanol fuel cells. In subsequent work, using the reducing agent $NaBH_4$, composites of graphene nanosheets decorated by Pt nanoclusters were prepared via reduction of graphite oxide and H_2PtCl_6 in one pot [73]. The electrochemically active surface area (ECSA) of the graphene-based catalyst is 44.6 $m^2\ g^{-1}$ while that of Pt/Vulcan is 30.1 $m^2\ g^{-1}$, and further, the graphene-based catalyst shows superior catalytic performance toward methanol oxidation (Fig. 2) [73]. An alternative synthesis approach, the rapid microwave method, was also used to produce a reduced graphene oxide supported Pt [74]. It is also found that the increased hydroxyl species on the catalysts makes it CO resistant. Besides the direct methanol or ethanol fuel cells, graphene-supported platinum also shows the higher electrocatalytic activity toward oxygen reduction [76].

In addition to work with single-metal catalysts, bimetallic Pt–Ru nanoparticles have been synthesized on graphene sheets using the EG reduction method [77] an6.2d impregnation method [78].

Results showed that graphene-supported Pt and Pt–Ru nanoparticles demonstrate enhanced performance over the widely used Vulcan XC-72R carbon black supported

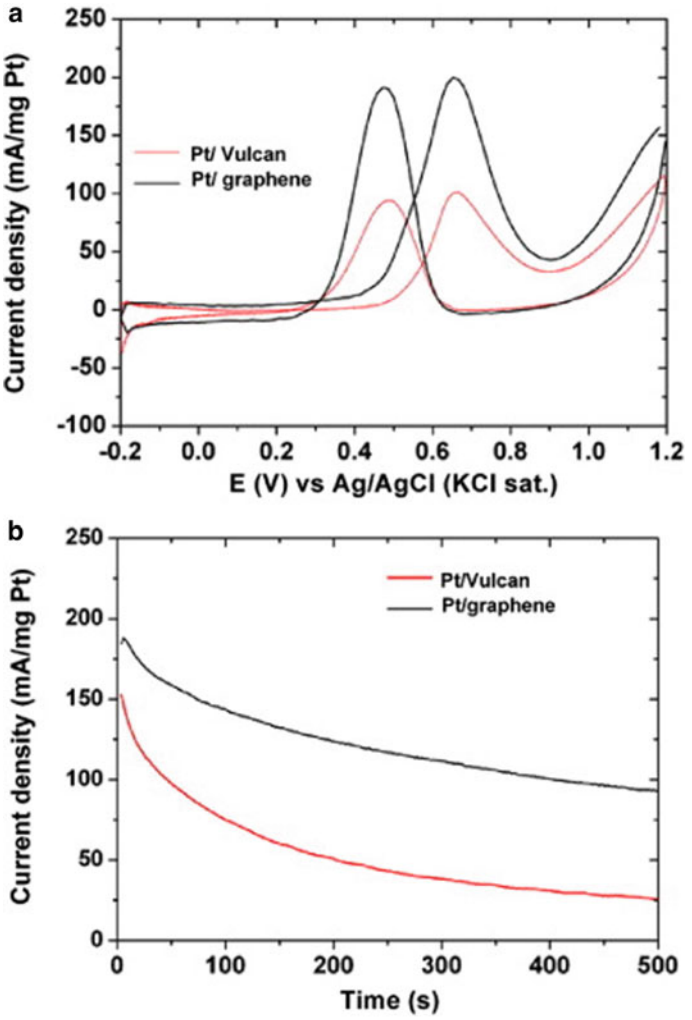

Fig. 2 Enhanced electrochemical activity toward methanol: **a** CV for Pt/graphene and Pt/Vulcan in nitrogen saturated aqueous solution of 0.5 M H_2SO_4 containing 0.5 M CH_3OH at a scan rate of 50 mV s^{-1}; **b** Chronoamperometric curves for the catalysts in the same solution at 0.6 V versus Ag/AgCl. (Reproduced with permission from ref [73]. Copyright © 2009 Elsevier B.V.)

catalyst for both methanol and ethanol electro-oxidation with regard to diffusion efficiency, oxidation potential, forward oxidation peak current density, and the ratio of the forward peak current density to the reverse peak current density [77]. Using the metal precursors (PtCl2 and RuCl3) and the solvent tetrahydrofuran(THF), a Pt–Ru catalyst with a high metal content of 80 wt.% was synthesized on the graphene sheets and showed superior electrochemical activity toward methanol oxidation compared with Pt–Ru/Vulcan XC-72R [78]. The enhanced catalytic activity was attributed to

the higher utilization and activation of Pt or Pt–Ru on graphene sheets because of the higher specific surface area of graphene sheets which leads to higher dispersion and better accessibility of Pt nanoparticles. From the preceding results, it appears that the higher electrochemical performance of graphene-supported catalysts is associated with the use of single-layer (high specific surface area) graphene sheets in the production of the catalyst. Confirmation that the superior electrocatalytic activity arises from the large surface area could be established by systematic studies of Pt nanoparticles dispersed on graphene sheets with tailored specific surface areas.

The enhanced electrocatalytic activity of graphene-supported catalysts may also be attributable to the grapheme microstructure such as the functional groups and defects as well as to the interaction of Pt clusters with graphene.

This hypothesis is supported by work that shows that functionalized graphene-supported Pt shows a higher electrochemical surface area and oxygen reduction activity as compared with commercial catalysts [79]. It was suggested that the graphene surface groups such as epoxy might function as anchoring sites for Pt precursors to prevent the aggregation of the Pt nanoparticles. This effect could contribute to improved dispersion of Pt nanoparticles on graphene sheets thus giving rise to the enhanced catalytic properties of the Pt cluster [79].

Another interesting finding, demonstrated through scanning transmission electron microscopy (STEM) studies, is that Pt particles below 0.5 nm in size are formed on grapheme sheets as illustrated in Fig. 3 [80]. The small Pt particles were confirmed by high-angle annular dark-field (HAADF) image and energy dispersive X-ray spectroscopy (EDS). This graphene-supported Pt was synthesized from the platinum precursor Pt $(NO_2)_2$_$(NH3)_2$ and from chemically reduced graphene using

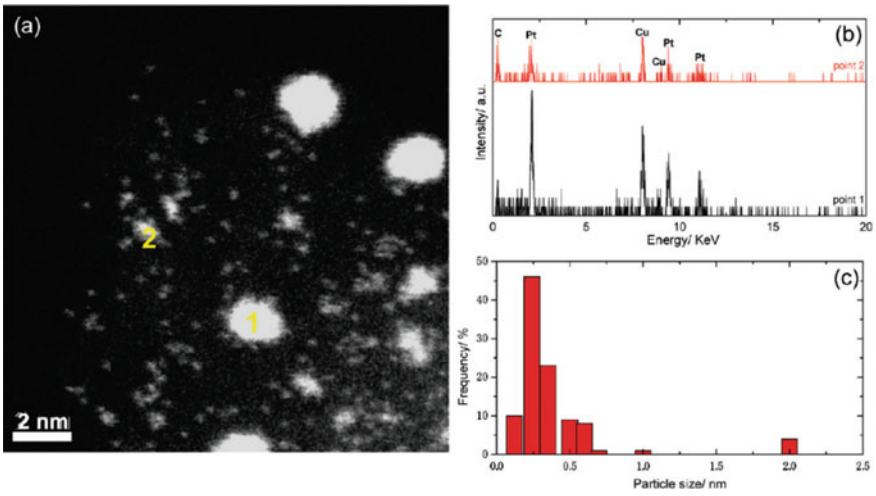

Fig. 3 Pt particles on the graphene sheets under STEM and Pt particles below 0.5 nm in size are observed: **a** HAADF image; **b** EDS spectrum; **c** Pt particle distribution. (Reproduced with permission from ref [80]. Copyright © 2009 American Chemical Society)

the impregnation method (Ar/H_2 at 400 °C). The resulting graphene-supported catalyst reveals an unusually high activity for methanol oxidation reaction compared to Pt/carbon black catalyst [80].

The author ascribed this enhanced electrocatalytic activity to the formation of dramatically smaller Pt particles. It is speculated that the strong interaction between Pt and graphene is responsible for the small Pt particles and thus might cause modulation in the electronic structure of the Pt clusters.

Unlike carbon supports (e.g., activated carbons), grapheme cannot exhibit micropores and deep cracks were deposited Pt nanoparticles would be isolated from the ionomer phase and thus unable to form electrochemically active TPBs. But carbon vacancies may exist in the produced graphene, especially in the chemically reduced graphene, where more charge, dangling bond, and functional groups can be entrapped. These features could lead to different localized electronic structures in the graphene sheets and interactions with catalyst precursors or metal clusters and therefore may impact the electrocatalytic activity. Interestingly, the relation of the peak current density and the scan rate in the cyclic voltammograms indicates that methanol diffuses faster on the surfaces of graphene sheets than that on the carbon black and graphite substrate [77].

Some of the preceding experimental studies are supported by theoretical studies showing that Pt bonds more strongly to functionalized graphene surfaces. From density functional theory (DFT) calculations, the gap between the highest occupied and lowest unoccupied molecular orbitals (the HOMO–LUMO gap) of hydrogen-terminated graphene is smaller than the zero-gap in infinite-size graphene. The small HOMO–LUMO gap is still retained after a Pt cluster binds to an edge of an sp^2 C surface to form two Pt–C bonds [81]. This theoretical calculation demonstrates that Pt clusters bond more strongly to the surface of the hydrogen-terminated graphene than to infinite-size graphene and that Pt clusters prefer the edge over the surface in the hydrogen-terminated graphene. In addition, oxygen-containing functional groups will not only function as anchoring sites for Pt precursors but also influence the position of the Pt cluster on the graphene sheets and the bonding energy with the sp^2 carbon in the graphene.

Further research is needed to understand the mechanism by which electrocatalytic activity is enhanced on graphene support. Specifically, studies comparing the performance of catalysts supported on defect-free and defect-rich graphene could help to explain the role of defects in the electrocatalytic activity. Likewise, systematic control of surface functional groups or of electronic structure (using nitrogen or boron doping) could yield a deeper understanding of the relative influence of these features and suggest areas for further improvement of graphene-supported catalysts.

4.1.2 Enhanced Durability

The unique structure of graphene may improve electrode durability by strengthening the interaction between the catalyst particles and the grapheme support. Using the accelerated degradation test (ADT) methods (potential step 1.4 V for 10 s to 0.85 V

for 5 s), a poly (diallyldimethylammonium chloride) (PDDA) modified graphene-supported Pt was compared to Pt/CNT and E-TEK Pt/C [82]. After 46 h of testing, Pt/CNT and E-TEK Pt/C degraded by 75% based on both ECSA and oxygen reduction reaction (ORR), but graphene-supported Pt only degraded only 40% (ECSA) and 20% (ORR). In this test, the Ptmorphology did not change, and the improved durability can be attributed to more stable graphene support. In another durability test, Pt morphology did change and the influence of the support on the morphological stability was investigated [79]. After 5000 cycles of 0.6 to 1.1 V ADT, the average Pt particle size in a graphene-supported catalyst increased from 2 to 5.5 nm and more than 75% of the Pt particles remained smaller than 6.9 nm. For E-TEK carbon-supported catalysts, the average particle increased from 2.8 to 6.9 nm, and more than 45% of the particles were over 6.9 nm (Fig. 4). This result indicates that the interaction of Pt with graphene is stronger than the interaction with the E-TEK carbon support, thus leading to less Pt sintering on grapheme than on E-TEK carbon. The different observations between this study and the former study regarding Pt morphology changes may be attributable to the use of the reduction preparation method in the former study and of the impregnation heat treatment method in the latter study. In other words, the use of H_2 and high temperature also changes the structure

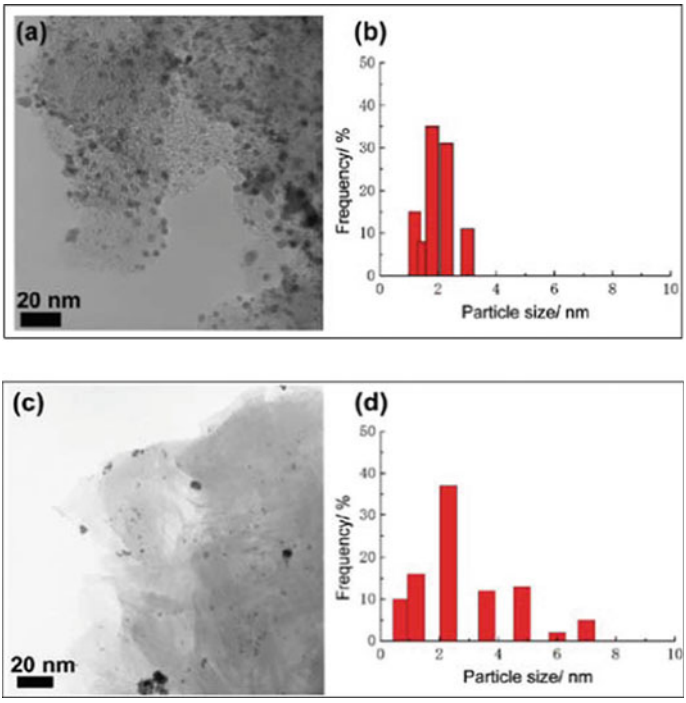

Fig. 4 TEM images of **a** E-TEK and **c** Pt-Graphene after 5000 CV degradation, and Pt nanoparticle size distribution diagrams on **b** E-TEK and **d** Pt-Graphene after 5000 CV degradation. (Reproduced with permission from ref [80]. Copyright © 2009 American Chemical Society)

of graphene sheets, creating H terminated graphene, and thus enhancing the Pt-sp^2 carbon bonding. As calculated by DFT, H terminated graphene has the advantage of enhancing the interactions between a Pt6 cluster and asp2 carbon surface [81].

As noted previously, nitrogen and boron can also be used to modify the electronic structure of the carbon support materials, thus improving the electrocatalytic activity and catalyst durability. The binding energy between a single platinum atom and several nitrogen-doped carbon grapheme structures was evaluated using DFT [83]. The nitrogen doping can double the binding energy, with the increase in binding energy proportional to the number and proximity of nitrogen atoms to the carbon-platinum bond. It should be noted that the addition of N atoms increases the number of dislocations in the lattice because N is prone to form pentagonal defects in the graphene structure [83].

4.1.3 Graphene-Based Electrodes

The use of 2-D grapheme as the catalyst support material in PEM fuel cells also creates opportunities to improve the structure of the catalyst layer although doing so requires consideration of the full range of catalyst layer properties-ionic transport, charge transport, and reactant transport in addition to ECSA. For example, one study has demonstrated an increase of nearly 80% in ECSA by further heat treatment of the catalyst (300 1C, 8 h).However, the fuel cell performance is lower than the untreated done, in which graphene-supported Pt-based fuel cell shows a maximum power of 161 mW cm^{-2} [76]. This can be attributed to the loss of proton conductivity of the Nafion ionomer in the catalyst layer during higher temperature treatment. Another key consideration in the development of graphene-based electrodes is the maintenance of good electronic conductance between graphene layers. As discussed above, nanostructured Pt particles dispersed on functionalized graphene can serve as spacers to prevent the re-agglomeration of graphene sheets. In addition, CNTs can be anchored on the graphene sheet to prevent face-to-face graphene agglomeration while simultaneously increasing the through-plane conductance. Polarization curves for the ORR in a PEM fuel cell electrode using a mix of graphene and CNT supported Pt as electrocatalysts exhibited performance of 540 mW cm-2 for the optimal case of equal fractions of each support (i.e., Pt/(50 wt.% graphenes + 50 wt.% CNT) [84]. This electrode structure is a combination of functionalized hybrid nanomaterials including three-, two-, and one-dimensional materials. While presenting some advantages, it is likely that the Pt/graphene sheets in this particular architecture pack together to form interstitial pores between the graphene sheets that are relatively inaccessible to electrolyte thus limiting the formation of TPBs. Recently, 3-D Pt-on-Pd bimetallic nanodendrites supported on graphene nanosheets have been constructed, representing a new type of graphene/metalhetero structure [85]. This structure, which exhibits a high electrochemically active area, consists of small single-crystal Pt nanoparticles supported on a Pd/graphene nanosheet with porous structure and good dispersion. Electrochemical tests show that the graphene/bimetallic nanodendrites hybrids demonstrate much higher electrocatalytic activity toward methanol oxidation than

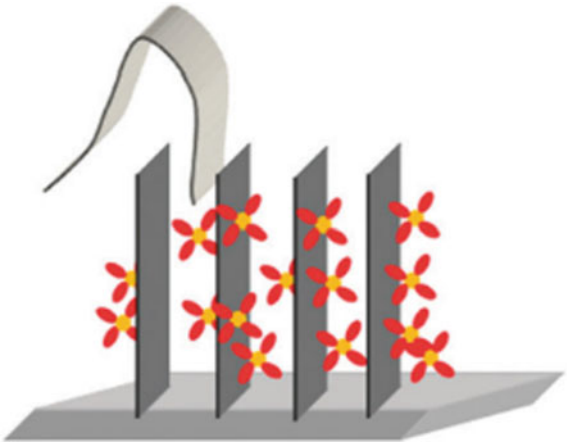

Fig. 5 Strategy for novel electrode structure: bimetallic nanodendrite hybrid catalyzed graphene sheets can be covered by a thin proton ionomer film and assembled on the proton electrolyte membrane. (Reproduced with permission from ref [86]. Copyright© the Owner Societies 2011)

either platinum black (PB) or commercial E-TEK Pt/C catalysts [85]. Furthermore, as illustrated in Fig. 5, the bimetallic nanodendrites can be applied to construct a novel electrode structure based on graphene nano sheets, which could fully realize the benefit of 2D graphene while avoiding its disadvantage. The bimetallic nanodendrite hybrid catalyst can be deposited on the graphene sheets. Then, the catalyzed graphene sheets can be assembled onto the PEM in well-ordered macroscopic arrays using directional flow techniques [84]. A very thin ionomer film can then be sprayed onto the arrays to form the ionic pathway. This ideal structure provides for electron transport along with the graphene sheet and ion transport in the parallel electrolytic film connecting the membrane to reaction sites. In this structure, control of the distance between the graphene sheets is critical to gas and water transport. Compared to the traditional electrode structure, TPBs are much more accessible as there is no agglomerate structure, and catalyst utilization is improved.

4.1.4 Emerging Applications for Graphene in Fuel Cells

Graphene doped by nitrogen can function as a metal-free catalyst for the oxygen reduction reaction (ORR). In a recent study, nitrogen-doped graphene (N-graphene) was synthesized by chemical vapor deposition of methane in the presence of ammonia. As illustrated in Fig. 5.9, the resulting N-graphene shows a much better electrocatalytic activity, long-term operational stability, and tolerance to CO than platinum for the ORR [87]. According to an earlier report on CNTs doped by nitrogen, [88], carbon atoms adjacent to nitrogen dopants possess a substantially high positive charge density to counterbalance the strong electronic affinity of the nitrogen atom. A redox cycling process reduces the carbon atoms that naturally exist in an oxidized form, followed by reoxidation of the reduced carbon atoms to their preferred oxidized state upon O_2 absorption [88]. This is the ORR mechanism on

the N-doped carbon electrodes. At the same time, the N-induced charge delocalization can change the chemisorption mode of O_2 and weaken the O–O bonding to facilitate ORR at the electrodes. Other work has also demonstrated, enhanced electrochemical activity and durability toward ORR on nitrogen-doped graphene [89]. The development of efficient, low cost, and stable N-doped graphene or CNT electrodes capable of replacing the expensive platinum-based electrocatalysts for ORR would be a revolutionary advance in PEM fuel cell technology.

Graphene sheets can also be used as composite fillers and conductive coating in fuel cell applications. PEM fuel cell performance can be improved by reducing ohmic losses in the membrane by either increasing ionic conductivity or decreasing the thickness of the membrane. Decreasing membrane thickness also facilitates water back diffusion allowing the anode to be operated without external humidification. But, the strength of the membranes becomes lower with the decrease in thickness. As a result, very thin membranes can bere inforced using polytetrafluoroethylene (PTFE) or CNT fillers. Graphene has a very high Young's modulus (B1.0 TPa) and could be used to reinforce the PEMs to dramatically increase their mechanical strength provided electrical shorting through the membrane can be avoided. Another potential application for graphene is as a coating on the bipolar plates to decrease the contact resistance and protect the plate material. Graphene is stable in the fuel cell environment and exhibits high thermal conductivity and electronic conductivity, and thus is potentially suitable for this application.

5 Electrospinning of Graphene

Electrospinning has emerged over the last decade as a promising nanotechnology-based approach to the design and development of intelligent and ultra-sensitive sensing systems [90]. The electrospinning technique is an effective method to produce nanofibres, nanobelts, Janus nanofibers, Janus nanobelts, hollow nanofibers, coaxial nanofibers, and coaxial nanoribbons with diameters ranging from micrometers to several nanometers using a wide variety of materials and improve the uniform dispersion of fillers and can also realize the effective alignment of fillers along with the oriented polymeric fibers [91, 92]. The electrospinning process consists of a high voltage power supply, a syringe pump, a metallic spinneret, and a conductive collector, as shown in Fig. 6 [90].

Graphene is usually hard to disperse uniformly in a polymeric matrix, graphene sheets tend to aggregate due to attractive van der Waals forces. Therefore, electrospinning requires that the graphene sheets first be dispersed in the polymer solution [93].

Composite fibers can be made mainly by two processes: mixing and spinning as shown in Fig. 7. Graphene can be incorporated during the mixing process in three different ways: solvent mixing, melt processing, and in-situ polymerization. Some researchers, after the spinning process, have tried to coat graphene onto the

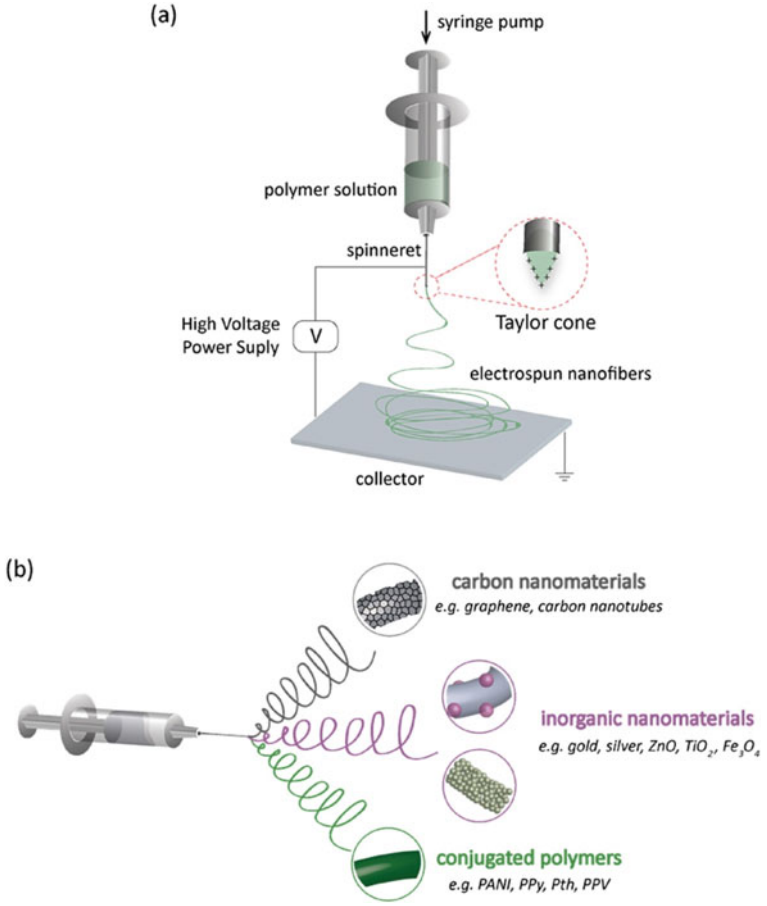

Fig. 6 Schematic diagram of **a** a typical electrospinning apparatus setup and **b** the electrospinning of multifunctional nanofibers containing different types of materials (Reproduced with permission from ref [90]. Copyright© 2017 Elsevier B.V.)

fiber surface. There are also different spinning methods to prepare graphene/polymer fibers: wet spinning, melt spinning, and electrical spinning [94].

Compared with traditional manufacturing methods (such as melt blending, solvent blending, and in-situ polymerization…, etc.), electrospinning is an ideal way to align carbon nanomaterials because of its simplicity and low cost of the processing system, the short time required to prepare continuous 1D structures and its versatility, which allows the preparation of fibers and membranes with a wide range of morphologies and materials [90–92]

Wang et al. [95] prepared the PVA/GO/TiO_2 core–shell fibers after electrospinning GO/PVA nanofibers as shown in Fig. 8. The experimental results showed that GO-doping decreased the temperature of decomposition and elongation at break

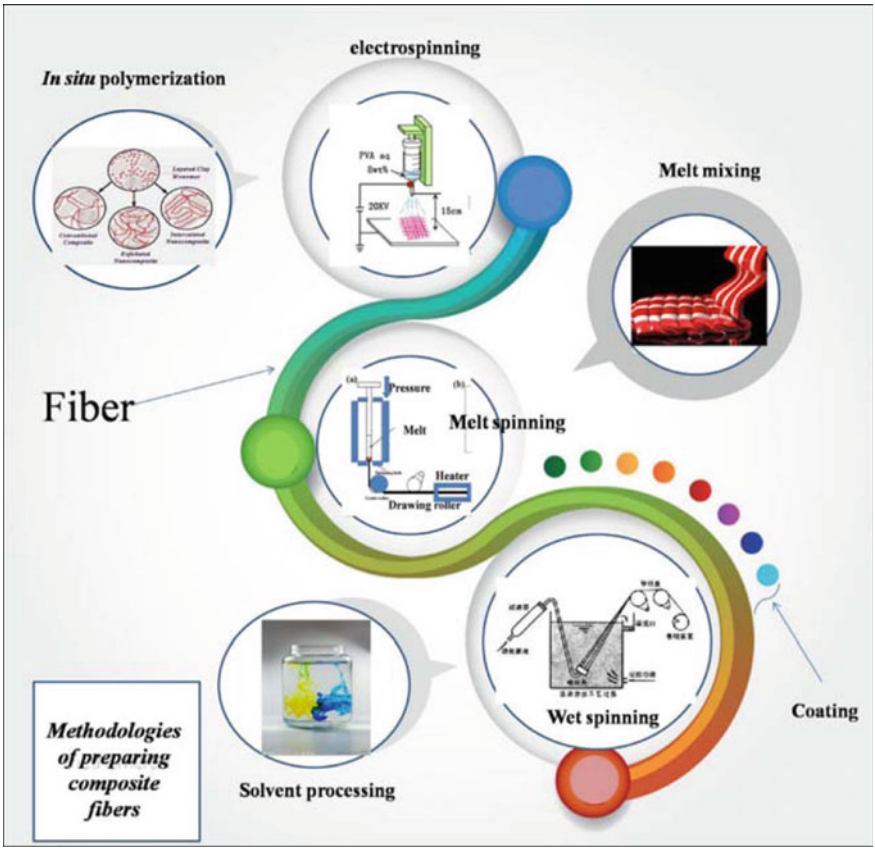

Fig. 7 Schematic illustration of the methods for the preparation of fiber composite. (Reproduced with permission from ref [94]. Copyright© 2016 Elsevier Ltd)

of PVA nanofibers, while, the degree of crystallinity and tensile strength increased Fig. 7c.The GOdoped PVA nanofibers can be used as a hard template to promote the growth of TiO_2. In addition, the PVA fibers, reinforced with both graphene and CNTs by dispersing graphene and CNTs into an aqueous PVA solution then spinning and demonstrated a strong synergistic effect by hybridization of single-walled carbon nanotubes (SWCNT) andRGO flakes [96].

Pan et al. [97] have reinforced Nylon fibers by graphene. Nylon-6 spider-wave-like nano-nets are manufactured by regulating the amount of GO in polymer solution during the electrospinning process as shown in Fig. 9a. The spider-wave-like nano-nets that comprise interlinked thick fibers (192 nm diameter) and thin (14 nm diameter) are widely distributed throughout the mat when the nylon-6 solution is reinforced with GO (Fig. 8c). The heterogeneous composite mats were composed of two nanofibers with different diameters in which pore diameter was greatly decreased by the factor of 2 compared to the pristine nylon-6 mat. The acceleration in ionization

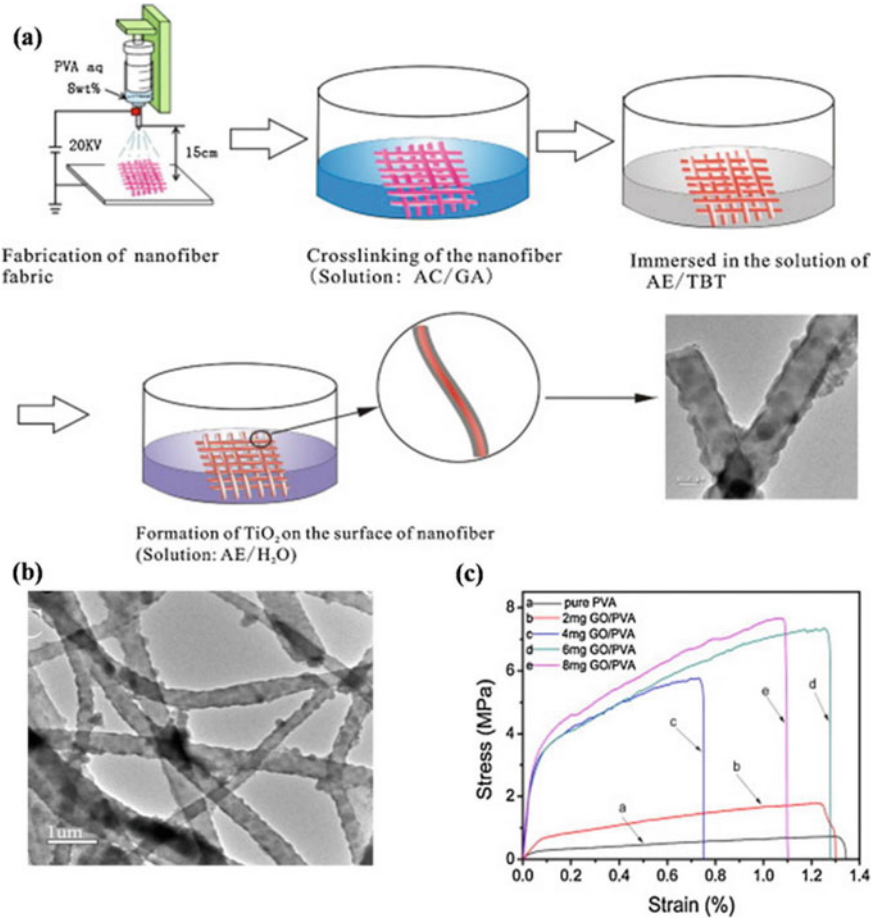

Fig. 8 The procedure for preparing of PVA/TiO_2 or PVA/GO/TiO_2 composite nanofibers through electrospinning and interface sol–gel reaction **a**. TEM images of composite nanofibers of PVA/GO/TiO_2**b**. Tensile stress–strain curves of nanofiber fabrics with various GO loading **c** .(Reproduced with permission from ref [95]. Copyright © 2014 Elsevier B.V.)

and degradation of nylon-6 (due to formic acid) solution caused by well-dispersed GO sheet as well as the formation of hydrogen bond between nylon-6 molecules and GO sheet during electrospinning are proposed as the possible mechanisms for the formation of these spider-wave-like nano-nets. Mack et al. designed a reinforced polymer composite by adding 1–4% graphite nanoplatelets into a PAN solution. Electrospinning produced composite nanofibers with average diameters of 300 nm. The composite nanofibers demonstrated a modest increase in thermal stability with increasing weight-percent graphite nanoplatelets [98].

He et al. [99] have prepared a new and special NaAlg fiber and added GO using a wet-spinning method. The NaAlg/GO fibers are nontoxic to cells which demonstrated

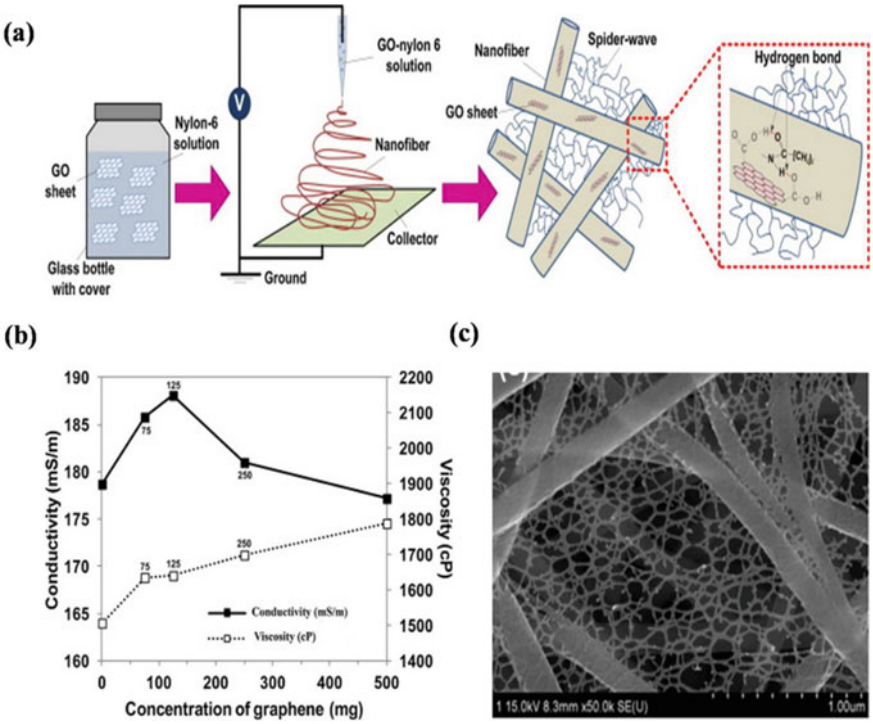

Fig. 6.9 Fabrication of spider-wave-like nano-nets and interaction of GO sheets and nylon-6 molecules by hydrogen bonding **a**. Conductivity and viscosity of GO containing nylon-6 solutions mats **b**. FE-SEM images of 125 mg GO containing nylon-6 solutions mats. (Reproduced with permission from ref [97]. Copyright © 2012 Elsevier B.V.)

the potential applications of the as-spun fibers in wound dressing materials. Li and co-workers [100], prepared a novel environmentally friendly adsorbent, calcium alginate (CA) immobilized GO fiber. Thermodynamic analysis proved that the adsorption reaction of methylene blue onto CA immobilized GO fiber was exothermic and spontaneous in nature.

Yoon et al. [101], prepared reinforced nanofibers of poly(D, L-lactic-co-glycolic acid) (PLGA) by adding 2-dimensional nanoscale fillers of GO nanosheets to PLGA nanofibers. Lamastra et al. [102], reinforced poly(e-caprolactone) (PCL) fibers with CNTs and graphene nanoplatelets (GNPs). CNTs and GNPs were accurately disentangled and dispersed in N, N-Dimethylformamide (DMF) by means of sonication, followed by electrospun with a mean diameter ranging between 1 and 2 μm. Asmatulu and co-workers [103], have fabricated PS and polyvinyl chloride (PVC) fibers incorporated TiO_2nanoparticles and graphene nanoflakes with an electrospinning technique, and then the surface morphology and super-hydrophobicity of these electrospun nanocomposite fibers were investigated. GO/chitosan composite fibers

were prepared by a wet spinning method, and their mechanical and absorption properties were investigated [104, 105]. Regenerated cellulose (RC) fibers filled with low graphene loading were also prepared, 50% improvement of tensile strength and 25% enhancement of Young's modulus were obtained [105]. Composite nanofibers of GO and gelatin were recently studied in Panzavolta's group. Young's modulus and fracture stress increased with the increasing content of GO [106].

Li et al. [107] employed the electrospinning technique to directly fabricate PVA and nanoscale graphene (NG)-based hybrid membranes doped with highly dispersed AgNPs (Fig. 6.10). Firstly, they conjugated the AgNPs onto NG sheets by self-assembly, and then, the NGeAgNP nanohybrids were electrospun with PVA solution. Compared to the PVA/AgNPs nanofibers, the introduction of nanographene promoted the dispersion of AgNPs in the PVA nanofibers. Due to the high-loading amounts and uniform dispersity of AgNPs, the PVA/ NG/AgNPs nanostructure showed significantly improved catalytic properties toward hydrogen peroxide. Promphet et al. [108] used electrospinning to develop graphene/ polyaniline/polystyrene (G/PANI/PS) nanoporous fiber modified screen-printed electrodes (SPE) for simultaneous determination of Pb(II) and Cd(II). The authors showed that due to the increase of the specific surface area of the electrospun G/PANI/PS nanoporous fibers, the electrochemical sensitivity of modified SPE was enhanced by a factor of three compared

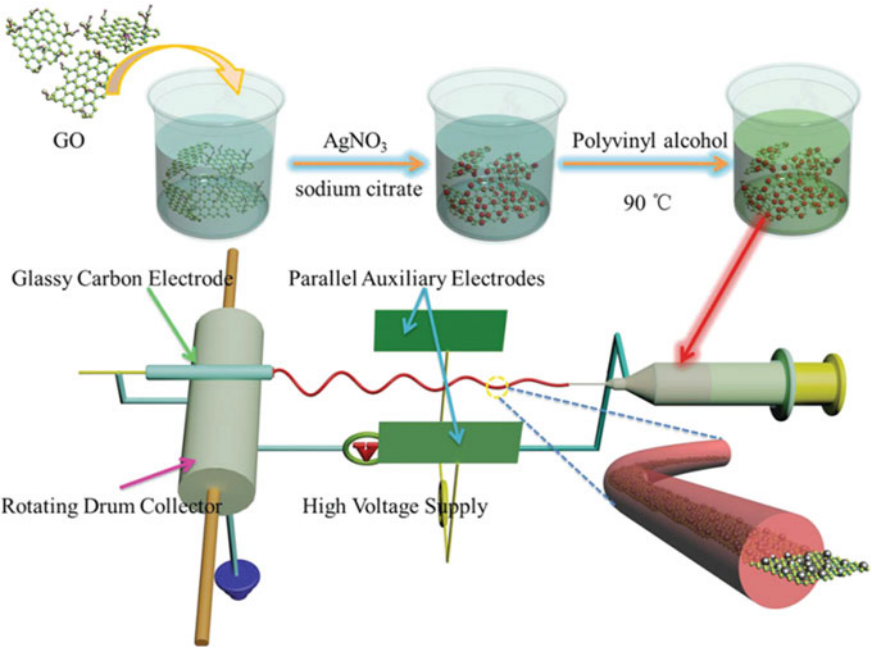

Fig. 6.10 Schematic representation for the fabrication mechanism of NG/AgNP hybrid membrane. (Reprinted with permission from ref [109]. Copyright© 2016 WILEY VCH Verlag GmbH & Co. KGaA, Weinheim)

to an unmodified SPE. Under optimal conditions, a linear relationship was found in a range of 10–500 μg L^{-1} with detection limit (S/N = 3) of 3.30 and 4.43 μg $L^{-1}$for Pb(II) and Cd(II), respectively. By simple washing step, the ESNFs-based electrode could be reused for more than ten replicates with high reproducibility for the determination of heavy metals in real river water samples.

Abideen et al. [110] developed a gas sensor platform assembling reduced graphene oxide (rGO) in ZnO ESNFs membrane (Fig. 6.10). Microstructural investigation revealed that the addition of rGO does not affect the size of the ZnO nanoparticles or nanofibers. The sensor response to 5 ppm NO_2 gas was increased by the addition of rGO to ZnO nanofibers. Overall, the rGO-loaded ZnO ESNFs showed higher sensitivity to different oxidizing and reducing gases compared to monolithic ZnO nanofibers (Fig. 6.11).

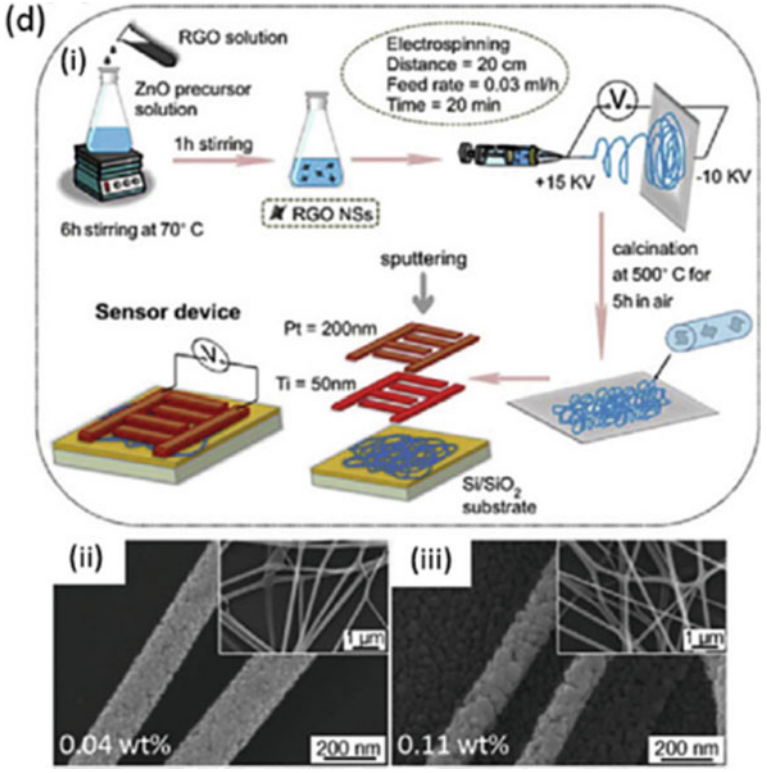

Fig. 6.11 The synthesis of rGO-loaded ZnO nanofibers via electrospinning method, (ii) and (iii) SEMimages of calcined rGO-loaded ZnO NFs. (Reprinted with permission from ref [110]. Copyright © 2015 Elsevier B.V.)

6 Conclusions

Graphene-based polymer nanocomposites have attracted a great deal of interest due to its good stability, interesting electroactivity, high capacitance, and unusual doping/de-doping chemistry, especially when combined with graphene, performance of nanocomposites is greatly improved. Therefore, graphene-based polymer nanocomposites can be widely employed in various applications.

In the field of electrochemical energy conversion and storage, graphene-based polymer nanocomposites have shown promise for applications in fuel cells, supercapacitors, and lithium-ion batteries. Due to its specific surface area and the presence of functional groups, edges, and defects, graphene-based electrodes demonstrate enhanced performance for such electrochemical energy devices.

In this book chapter, many aspects of graphene-based polymer nanocomposites have been discussed: preparation methods, some applications in polymer composites examples, and graphene-based electrochemical energy devices application especially the fuel cells.

The choice of preparation methods is determined by the surface functionalization of integrated graphitic sheets. Thus, the key to preparing advanced graphene-based nanocomposites is the engineering at the polymer-graphene interface.

The fuel cell domain application of graphene in polymer nanocomposite was reviewed. This study summarized the research efforts to take advantage of the unique features of graphene to produce supported catalysts with enhanced activity, increased durability, and high-performance electrode architectures, the development for enhanced fuel cell catalysts through the use of a high specific surface area graphene support was explored by preparing graphene–metal particle nanocomposites and the investigation of the enhanced durability where the unique structure of graphene may improve electrode durability by strengthening the interaction between the catalyst particles and the graphene support.

Electrospinning technique has evolved significantly since it was first suggested, in the last decade it has proven to be a powerful method for making distinct functional nanomaterials for non-medical, medical applications and especially in textile applications, optical devices, membranes, sensors, tissue engineering.

References

1. Novoselov, K.S., et al.: Electric field effect in atomically thin carbon films. Science **306**(5696), 666–669 (2004)
2. Geim, A.K., Novoselov, K.S.: The rise of graphene. Nat. Mater. **6**(3), 183–191 (2007)
3. Geim, A.K.: Graphene: status and prospects. Science **324**(5934), 1530–1534 (2009)
4. Stankovich, S., et al.: Graphene-based composite materials. Nature **442**(7100), 282–286 (2006)
5. Ramanathan, T., et al.: Functionalized graphene sheets for polymer nanocomposites. Nat. Nanotechnol. **3**(6), 327–331 (2008)

6. Dikin, D.A., et al.: Preparation and characterization of graphene oxide paper. Nature **448**(7152), 457–460 (2007)
7. Kim, K.S. et al.,: Large-scale pattern growt.h of graphene films for stretchable transparent electrodes. Nature **457**(7230), 706–710 (2009)
8. Reina, A., et al.: Large area, few-layer graphene films on arbitrary substrates by chemical vapor deposition. Nano Lett. **9**(1), 30–35 (2009)
9. Shi, Y.M., et al.: Work function engineering of graphene electrode via chemical doping. ACS Nano **4**(5), 2689–2694 (2010)
10. Li, X.S., et al.: Transfer of large-area graphene films for highperformance transparent conductive electrodes. Nano Lett. **9**(12), 4359–4363 (2009)
11. Bunch, J.S., et al.: Electromechanical resonators from graphene sheets. Science **315**(5811), 490–493 (2007)
12. Chen, C.Y., et al.: Performance of monolayer graphene nanomechanical resonators with electrical readout. Nat. Nanotechnol. **4**(12), 861–867 (2009)
13. Schedin, F., et al.: Detection of individual gas molecules adsorbed on graphene. Nat. Mater. **6**(9), 652–655 (2007)
14. Elias, D.C., et al.: Control of graphene's properties by reversible hydrogenation: evidence for graphane. Science **323**(5914), 610–613 (2009)
15. Shan, C.S., et al.: Direct electrochemistry of glucose oxidase and biosensing for glucose based on graphene. Anal. Chem. **81**(6), 2378–2382 (2009)
16. Balog, R., et al.: Bandgap opening in graphene induced by patterned hydrogen adsorption. Nat. Mater. **9**(4), 315–319 (2010)
17. Stoller, M.D., et al.: Graphene-based ultracapacitors. Nano Lett. **8**(10), 3498–3502 (2008)
18. Kouni, B., Belhamdi, H.: In: Surface Engineering of Graphene, pp. 231257. Springer (2019)
19. Wang, L., Lu, X., Lei, S., Song, Y.: Graphene-based polyaniline nanocomposites: preparation, properties and applications. J. Mater. Chem. A **2**, 4491 (2014)
20. Xu, Y., Wang, Y., Jiajie, L., Huang, Y., Ma, Y., Wan, X., Chen, Y.: A hybrid material of graphene and poly (3, 4-ethyldioxythiophene) with high conductivity, flexibility, and transparency. Nano Res **2**, 343–348 (2009)
21. Quan, H., Zhang, B., Zhao, Q., Yuen, R.K.K., Li, R.K.Y.: Facile preparation and thermal degradation studies of graphite nanoplatelets (GNPs) filled thermoplastic polyurethane (TPU) nanocomposites. Composites A **40**, 1506–1513 (2009)
22. Eda, G., Chhowalla, M.: Graphene-based composite thin films for electronics. Nano Lett **9**, 814–818 (2009)
23. Liang, J., Xu, Y., Huang, Y., Zhang, L., Wang, Y., Ma, Y., Li, F., Guo, T., Chen, Y.: Infrared-triggered actuators from graphene-based nanocomposites. J. Phys. Chem. **113**, 9921–9927 (2009)
24. Kim, H., Macosko, C.W.: Processing–property relationships of polycarbonate/graphene nanocomposites. Polymer **50**, 3797–3809 (2009)
25. Li, H., Pang, S., Wu, S., Feng, X., Mullen, K., Bubeck, C.: Layer-by-layer assembly and UV photoreduction of graphene-polyoxometalate composite films for electronics. J Am Chem Soc **133**, 9423–9429 (2011)
26. Cassagneau, T., Fendler, J.H.: High density rechargeable lithium-ion batteries self-assembled from graphite oxide nanoplatelets and polyelectrolytes. Adv Mater **10**, 877–881 (1998)
27. Hu, H., Wang, X., Wanga, J., Wana, L., Liu, F., Zheng, H., Chen, R., Xu, C.: Preparation and properties of graphene nanosheets-polystyrene nanocomposites via in situ emulsion polymerization. Chem Phys Lett **484**, 247–253 (2010)
28. Hu, K., Kulkarni, D.D., Choi, Vladimir V. Tsukruk.Graphene-polymer nanocomposites for structural and functional applications.Progress in Polymer Science 39 (2014) 1934–1972
29. Kalaitzidou, K., Fukushima, H., Drzal, L.T.: A new compounding method for exfoliated graphite-polypropylene nanocomposites with enhanced flexural properties and lower percolation threshold. Compos. Sci. Technol. **67**, 2045–2051 (2007)
30. Zheng, W., Lu, X., Wong, S.C.: Electrical and mechanical properties of expanded graphite-reinforced high-density polyethylene. J. Appl. Polym. Sci. **91**, 2781–2788 (2004)

31. Zhao, Y.F., Xiao, M., Wang, S.J., Ge, X.C., Meng, Y.Z.: Preparation and properties of electrically conductive PPS/expanded graphite nanocomposites. Compos. Sci. Technol. **67**, 2528–2534 (2007)
32. Du, X.S., Xiao, M., Meng, Y.Z.: Synthesis and characterization of polyaniline/graphite conducting nanocomposites. J. Polym. Sci. B Polym. Phys. **42**, 1972–1978 (2004)
33. Cho, D., Lee, S., Yang, G., Fukushima, H., Drzal, L.T.: Dynamic mechanical and thermal properties of phenylethynyl-terminated polyimide composites reinforced with expanded graphite nanoplatelets. Macromol. Mater. Eng. **290**, 179–87 (2005)
34. Kim, H., Miura, Y., Macosko, C.W.: Graphene/polyurethane nanocomposites for improved gas barrier and electrical conductivity. Chem Mater **22**, 3441–3450 (2010)
35. Steinert, B.W., Dean, D.R.: Polymer **50**(3), 898–904 (2009)
36. Bortz, D.R., Heras, E.G., Martin-Gullon, I.: Impressive fatigue life and fracture toughness improvements in graphene oxide/epoxy composites. Macromolecules **45**, 238–245 (2012)
37. Wajid, A.S., Ahmed, H.S.T., Das, S., Irin, F., Jankowski, A.F., Green, M.J.: Highperformance pristine graphene/epoxy composites with enhanced mechanical and electrical properties. Macromol. Mater. Eng. **298**, 339–347 (2012)
38. Galpaya, D., Wang, M., George, G., Motta, N., Waclawik, E., Yan, C.: Preparation of graphene oxide/epoxy nanocomposites with significantly improved mechanical properties. J. Appl. Phys. **116,** 053518 (2014)
39. Shen, X., Pei, X., Fu, S., Friedrich, K.: Significantly modified tribological performance of epoxy nanocomposites at very low graphene oxide content. Polymer **54**, 1234–1242 (2013)
40. Cooper, D.R., D'Anjou, B., Ghattamaneni, N., Harack, B., Hilke, M., Horth, A., Majlis, N., Massicotte, M., Vandsburger, L., Whiteway, E., Yu, V.: Experimental review of graphene. ISRN Condens. Mater. Phys. **2012**, 56 (2012)
41. Wei, J., Vo, T., Inam, F.: Epoxy/graphene nanocomposites—processing and properties: a review. RSC Adv. **5**, 73510–73524 (2015)
42. Sandler, J.K.W., Kirk, J.E., Kinloch, I.A., Shaffer, M.S.P., Windle, A.H.: Ultra-low electrical percolation threshold in carbon-nanotube-epoxy composites. Polymer **44**, 5893–5899 (2003)
43. Zhao, S., Chang, H., Chen, S., Cui, J., Yan, Y.: High-performance and multifunctional epoxy composites filled with epoxide-functionalized graphene. Eur. Polymer J. **84**, 300–312 (2016)
44. Atif, R., Shyha, I., Inam, F.: Mechanical, thermal, and electrical properties of graphene-epoxy nanocomposites—a review. Polymers **8**, 281 (2016)
45. Kim, C., Khan, W., Kim, D., Cho, K., Park, S.: Graphene oxide/cellulose composite using NMMO monohydrate. Carbohydr. Polym. **86**, 903–909 (2011)
46. Luong, N.D., Pahimanolis, N., Hippi, U., Korhonen, J.T., Ruokolainen, J., Johansson, L., Nam, J., Seppälä, J.: Graphene/cellulose nanocomposite paper with high electrical and mechanical performances. J. Mater. Chem. **21**, 13991–13998 (2011)
47. Weng, Z., Su, Y., Wang, D., Li, F., Du, J., Cheng, H.: Graphene-cellulose paper flexible supercapacitors. Adv. Energy Mater. **1**, 917–922 (2011)
48. Xu, M., Huang, Q., Wang, X., Sun, R.: Highly tough cellulose/graphene composite hydrogels prepared from ionic liquids. Ind. Crops Prod. **70**, 56–63 (2015)
49. Zhao, X., Zhang, Q., Chen, D., Lu, P.: Enhanced mechanical properties of graphene-based poly(vinyl alcohol) composites. Macromolecules **43**, 2357–2363 (2010)
50. Liang, J., Huang, Y., Zhang, L., Wang, Y., Ma, Y., Guo, T., Chen, Y.: Molecular-level dispersion of graphene into poly(vinyl alcohol) and effective reinforcement of their nanocomposites. Adv. Funct. Mater. **19**, 2297–2302 (2009)
51. Lee, Y.R., Raghu, A.V., Jeong, H.M., Kim, B.K.: Properties of waterborne polyurethane/functionalized graphene sheet nanocomposites prepared by an in situ method. Macromol. Chem. Phys. **210**, 1247–1254 (2009)
52. Liang, J., Xu, Y., Huang, Y., Zhang, L., Wang, Y., Ma, Y., Li, F., Guo, T., Chen, Y.: Infrared-triggered actuators from graphene-based nanocomposites. J. Phys. Chem. C. **113**, 9921–9927 (2009)
53. Zhang, H., Zheng, W., Yan, Q., Yang, Y., Wang, J., Lu, Z., Ji, G., Yu, Z.: Electrically conductive polyethylene terephthalate/graphene nanocomposites prepared by melt compounding. Polymer **51**, 1191–1196 (2010)

54. Kim, H., Macosko, C.W.: Processing-property relationships of polycarbonate/graphene composites. Polymer **50**, 3797–3809 (2009)
55. Stankovich, S., Dikin, D.A., Dommett, G.H.B., Kohlhaas, K.M., Zimney, E.J., Stach, E.A., Piner, R.D., Nguyen, S.T., Ruoff, R.S.: Graphene-based composite materials. Nature **442**, 282–286 (2006)
56. Liu, N., Luo, F., Wu, H., Liu, Y., Zhang, C., Chen, J.: One-step ionic-liquid-assisted electrochemical synthesis of ionic-liquid-functionalized graphene sheets directly from graphite. Adv. Funct. Mater. **18**, 1518–1525 (2008)
57. Wang, R., Wang, S., Chen, S., Jiang, G.: In situ polymerization approach to poly(*E*-caprolactone)-graphene oxide composites. Design. Monom. Polym. **15**(3), 303–310 (2012)
58. Chieng, B.W., Ibrahim, N.A., Wan Yunus, W.M.Z.: Optimization of tensile strength of poly(lactic acid)=graphene nanocomposites using response surface methodology. Polym.-Plast. Technol. Eng. **51**(8), 791–799 (2012)
59. Liu, Q., Zhou, X., Fan, X., Zhu, C., Yao, X., Liu, Z.: Mechanical and thermal properties of epoxy resin nanocomposites reinforced with graphene oxide. Polym.-Plast. Technol. Eng. **51**(3), 251–256 (2012)
60. Mohamadi, S., Sanjani, N.S., Mahdavi, H.: Functionalization of graphene sheets via chemically grafting of PMMA chains through in situ polymerization. J. Macromol. Sci. Pt. A **48**(8), 577–582 (2011)
61. Liang, J., Huang, L., Li, N., Huang, Y., Wu, Y., Fang, S., Oh, J., Kozlov, M., Ma, Y., Li, F., Baughman, R., Chen, Y.: Electromechanical actuator with controllable motion, fast response rate, and highfrequency resonance based on graphene and polydiacetylene. ACS Nano **6**(5), 4508–4519 (2012)
62. Pan, B., Zhao, J., Zhang, Y., Zhang, Y.: Wear performance and mechanisms of polyphenylene sulfide=polytetrafluoroethylene wax composite coatings reinforced by graphene. J. Macromol. Sci. Pt. B Phys. **51**(6), 1218–1227 (2012)
63. Pang, H., Bao, Y., Lei, J., Tang, J.H., Ji, X., Zhang, W.Q., Chen, C.: Segregated conductive ultrahigh-molecular-weight polyethylene composites containing high-density polyethylene as carrier polymer of graphene nanosheets. Polym.-Plast. Technol. Eng. **51**(14), 1483–1486 (2012)
64. Hou, J., Shao, Y., Ellis, M.W., Moore, R.B., Yi, B.: Graphene-based electrochemical energy conversion and storage: fuel cells, supercapacitors and lithium ion batteries. Phys. Chem. Chem. Phys. **13**, 15384–15402 (2011)
65. Tang, L.H., et al.: Preparation, structure, and electrochemical properties of reduced graphene sheet films. Adv. Funct. Mater. **19**(17), 2782–2789 (2009)
66. Zhou, M., Zhai, Y.M., Dong, S.J.: Electrochemical sensing and biosensing platform based on chemically reduced graphene oxide. Anal. Chem. **81**(14), 5603–5613 (2009)
67. McCreery, R.L.: Advanced carbon electrode materials for molecular electrochemistry. Chem. Rev. **108**(7), 2646–2687 (2008)
68. Pumera, M.: Electrochemistry of graphene: new horizons for sensing and energy storage. Chem. Rec. **9**(4), 211–223 (2009)
69. Steele, B.C.H., Heinzel, A.: Materials for fuel-cell technologies. Nature **414**(6861), 345–352 (2001)
70. Borup, R., et al.: Scientific aspects of polymer electrolyte fuel cell durability and degradation. Chem. Rev. **107**(10), 3904–3951 (2007)
71. Shao, Y.Y., Yin, G.P., Gao, Y.Z.: Understanding and approaches for the durability issues of Pt-based catalysts for PEM fuel cell. J. Power Sources **171**(2), 558–566 (2007)
72. Xu, C., Wang, X., Zhu, J.W.: Graphene-metal particle nanocomposites. J. Phys. Chem. C **112**(50), 19841–19845 (2008)
73. Li, Y.M., Tang, L.H., Li, J.H.: Preparation and electrochemical performance for methanol oxidation of Pt/graphene nanocomposites. Electrochem. Commun. **11**(4), 846–849 (2009)
74. Sharma, S., et al.: Rapid microwave synthesis of CO tolerant reduced graphene oxide-supported platinum electrocatalysts for oxidation of methanol. J. Phys. Chem. C **114**(45), 19459–19466 (2010)

75. Hou, J.B., et al.: Electrochemical impedance investigation of proton exchange membrane fuel cells experienced subzero temperature. J. Power Sources **171**(2), 610–616 (2007)
76. Seger, B., Kamat, P.V.: Electrocatalytically active graphene platinum nanocomposites. role of 2-D carbon support in PEM fuel cells. J. Phys. Chem. C. **113**(19), 7990–7995 (2009)
77. Dong, L.F., et al.: Graphene-supported platinum and platinum ruthenium nanoparticles with high electrocatalytic activity for methanol and ethanol oxidation. Carbon **48**(3), 781–787 (2010)
78. Bong, S., et al.: Graphene supported electrocatalysts for methanol oxidation. Electrochem. Commun. **12**(1), 129–131 (2010)
79. Kou, R., et al.: Enhanced activity and stability of Pt catalysts on functionalized graphene sheets for electrocatalytic oxygen reduction. Electrochem. Commun. **11**(5), 954–957 (2009)
80. Yoo, E., et al.: Enhanced electrocatalytic activity of Pt subnanoclusters on graphene nanosheet surface. Nano Lett. **9**(6), 2255–2259 (2009)
81. Yumura, T., et al.: The use of nanometer-sized hydrographene species for support material for fuel cell electrode catalysts: a theoretical proposal. Phys. Chem. Chem. Phys. **11**(37), 8275–8284 (2009)
82. Shao, Y.Y., et al.: Highly durable graphene nanoplatelets supported Pt nanocatalysts for oxygen reduction. J. Power Sources **195**(15), 4600–4605 (2010)
83. Groves, M.N., et al.: Improving platinum catalyst binding energy to graphene through nitrogen doping. Chem. Phys. Lett. **481**(4–6), 214–219 (2009)
84. Jafri, R.I., et al.: Nanostructured Pt dispersed on graphenemultiwalled carbon nanotube hybrid nanomaterials as electrocatalyst for PEMFC. J. Electrochem. Soc. **157**(6), B874–B879 (2010)
85. Guo, S.J., Dong, S.J., Wang, E.W.: Three-dimensional Pt-on-Pd bimetallic nanodendrites supported on graphene nanosheet: Facile synthesis and used as an advanced nano electron catalyst for methanol oxidation. ACS Nano **4**(1), 547–555 (2010)
86. Hou, J. et al.: Graphene-based electrochemical energy conversion and storage: fuel cells, supercapacitors and lithium ion batteries. Phys. Chem. Chem. Phys. 15384 (2011)
87. Qu, L.T., et al.: Nitrogen-doped graphene as efficient metal-free electrocatalyst for oxygen reduction in fuel cells. ACS Nano **4**(3), 1321–1326 (2010)
88. Gong, K.P., et al.: Nitrogen-doped carbon nanotube arrays with high electrocatalytic activity for oxygen reduction. Science **323**(5915), 760–764 (2009)
89. Shao, Y.Y., et al.: Nitrogen-doped graphene and its electrochemical applications. J. Mater. Chem. **20**(35), 7491–7496 (2010)
90. Mercante, L.A., et al.: Electrospinning-based (bio)sensors for food and agricultural applications: a review. TrAC Trends Anal. Chem. **1**(91), 91–103 (2017)
91. Navarro-Pardo, F. et al.: Carbon nanotube and graphene-based polyamide electrospun nanocomposites: a review. J. Nanomater. (2016)
92. Guo, Y., et al.: Significantly enhanced and precisely modeled thermal conductivity in polyimide nanocomposites with chemically modified graphene via in situ polymerization and electrospinning-hot press technology. J. Mater. Chem. C. **6**(12), 3004–3015 (2018)
93. Das, S., et al.: Electrospinning of polymer nanofibers loaded with noncovalently functionalized graphene. J. Appl. Polym. Sci. **128**(6), 4040–4046 (2013)
94. Ji, X., et al.: Review of functionalization, structure and properties of graphene/polymer composite fibers. Compos. A Appl. Sci. Manuf. **1**(87), 29–45 (2016)
95. Wang, B., et al.: Fabrication of PVA/graphene oxide/TiO2 composite nanofibers through electrospinning and interface sol–gel reaction: Effect of graphene oxide on PVA nanofibers and growth of TiO_2. Colloids Surf. A **5**(457), 318–325 (2014)
96. Shin, M.K., et al.: Synergistic toughening of composite fibres by self-alignment of reduced graphene oxide and carbon nanotubes. Nat. Commun. **3**(1), 1–8 (2012)
97. Pant, H.R., et al.: Bimodal fiber diameter distributed graphene oxide/nylon-6 composite nanofibrous mats via electrospinning. Colloids Surf., A **5**(407), 121–125 (2012)
98. Mack, J.J., et al.: Graphite nanoplatelet reinforcement of electrospun polyacrylonitrile nanofibers. Adv. Mater. **17**(1), 77–80 (2005)

99. He, Y., et al.: Alginate/graphene oxide fibers with enhanced mechanical strength prepared by wet spinning. Carbohyd. Polym. **88**(3), 1100–1108 (2012)
100. Li, Y., et al.: Methylene blue adsorption on graphene oxide/calcium alginate composites. Carbohyd. Polym. **95**(1), 501–507 (2013)
101. Yoon, O.J., et al.: Nanocomposite nanofibers of poly (D, L-lactic-co-glycolic acid) and graphene oxide nanosheets. Compos. A Appl. Sci. Manuf. **42**(12), 1978–1984 (2011)
102. Lamastra, F.R., et al.: Poly (ε-caprolactone) reinforced with fibres of poly (methyl methacrylate) loaded with multiwall carbon nanotubes or graphene nanoplatelets. Chem. Eng. J. **1**(195), 140–148 (2012)
103. Asmatulu, R., Ceylan, M., Nuraje, N.: Study of superhydrophobic electrospun nanocomposite fibers for energy systems. Langmuir **27**(2), 504–507 (2011)
104. Li, Y., et al.: Mechanical and dye adsorption properties of graphene oxide/chitosan composite fibers prepared by wet spinning. Carbohyd. Polym. **15**(102), 755–761 (2014)
105. Tian, M., et al.: Enhanced mechanical and thermal properties of regenerated cellulose/graphene composite fibers. Carbohyd. Polym. **13**(111), 456–462 (2014)
106. Panzavolta, S., et al.: Structural reinforcement and failure analysis in composite nanofibers of graphene oxide and gelatin. Carbon **1**(78), 566–577 (2014)
107. Li, D., et al.: Nanofibers of conjugated polymers prepared by electrospinning with a two-capillary spinneret. Adv. Mater. **16**(22), 2062–2066 (2004)
108. Promphet, N., et al.: An electrochemical sensor based on graphene/polyaniline/ polystyrene nanoporous fibers modified electrode for simultaneous determination of lead and cadmium. Sens. Actuators B Chem. **1**(207), 526–534 (2015)
109. Li, Y., et al.: Nanoscale graphene doped with highly dispersed silver nanoparticles: quick synthesis, facile fabrication of 3D membrane-modified electrode, and super performance for electrochemical sensing. Adv. Func. Mater. **26**(13), 2122–2134 (2016)
110. Abideen, Z.U., et al.: Excellent gas detection of ZnO nanofibers by loading with reduced graphene oxide nanosheets. Sens. Actuators B Chem. **31**(221), 1499–1507 (2015)